



THE UNIVERSITY *of* EDINBURGH

## Edinburgh Research Explorer

# Improving the through-thickness electrical conductivity of carbon fiber reinforced polymer composites using interleaving conducting veils

### Citation for published version:

Waqas, M, Robert, C, Arif, U, Radacsi, N, Ray, D & Koutsos, V 2022, 'Improving the through-thickness electrical conductivity of carbon fiber reinforced polymer composites using interleaving conducting veils', *Journal of Applied Polymer Science*. <https://doi.org/10.1002/app.53060>

### Digital Object Identifier (DOI):

[10.1002/app.53060](https://doi.org/10.1002/app.53060)

### Link:

[Link to publication record in Edinburgh Research Explorer](#)

### Document Version:

Publisher's PDF, also known as Version of record

### Published In:

Journal of Applied Polymer Science

### General rights




Copyright for the publications made accessible via the Edinburgh Research Explorer is retained by the author(s) and / or other copyright owners and it is a condition of accessing these publications that users recognise and abide by the legal requirements associated with these rights.

### Take down policy

The University of Edinburgh has made every reasonable effort to ensure that Edinburgh Research Explorer content complies with UK legislation. If you believe that the public display of this file breaches copyright please contact [openaccess@ed.ac.uk](mailto:openaccess@ed.ac.uk) providing details, and we will remove access to the work immediately and investigate your claim.



# Improving the through-thickness electrical conductivity of carbon fiber reinforced polymer composites using interleaving conducting veils

Muhammad Waqas<sup>1</sup>  | Colin Robert<sup>1</sup> | Urwah Arif<sup>2</sup> | Norbert Radacsi<sup>1</sup> |  
Dipa Ray<sup>1</sup>  | Vasileios Koutsos<sup>1</sup> 

<sup>1</sup>School of Engineering, Institute for Materials and Processes, The University of Edinburgh, Edinburgh, UK

<sup>2</sup>School of Engineering, Institute of Bioengineering, Scottish Microelectronics Centre, The University of Edinburgh, Edinburgh, UK

## Correspondence

Dipa Ray, School of Engineering, Institute for Materials and Processes, The University of Edinburgh, King's Buildings, Edinburgh EH9 3FB, UK.  
Email: [dipa.roy@ed.ac.uk](mailto:dipa.roy@ed.ac.uk)

## Abstract

In this study, thin carbon fiber-based conducting veils were used as interleaving materials to improve the through-thickness electrical conductivity of carbon fiber reinforced composites. Carbon fiber (CF) or nickel-coated carbon fiber (NiCF) veils were used as interlayers between standard carbon fiber reinforcement fabrics. The through-thickness electrical conductivity of the interleaved composites with CF or NiCF veils improved over 50 fold, from 0.18 to 9.47 and 9.16 S/cm, respectively, compared to the control specimens. However, the interleaved specimens exhibited a ca. 20%–24% reduction in their interlaminar shear strength (ILSS) and flexural strength. The introduction of conducting veils facilitated establishing an electrical pathway between the carbon fabric plies by reducing the non-conducting resin rich zone in the interlaminar region. This established an electrically conductive pathway across the thickness of the laminate. This study reveals that conducting veil-interleaved composites can meet a functional integration requirement of the aerospace sector for electrical properties, and can find applications in lightning protection, EMI shielding, and structural health monitoring.

## KEYWORDS

CFRP composites, lightning strike protection, microscopy, through-thickness electrical conductivity, veil interleaved composites

## 1 | INTRODUCTION

Carbon-fiber reinforced polymer (CFRP) composites provide an alternative to traditional metal alloys for manufacturers and builders. The introduction of polymer composites in mainframes of modern structures, however, poses unique challenges and issues in terms of their multifunctional properties (e.g., electrical and thermal

conductivities), as well as the potential risk of interlaminar damage under impact and fatigue loading due to the brittle nature of the matrix resins.<sup>1,2</sup> Aircraft fuselages made from composites provide the best weight and electrical performance solution while lowering airline operations & maintenance expenses and carbon footprint. To achieve the same electrical and environmental (temperature, humidity, pressure) performance offered by the

This is an open access article under the terms of the [Creative Commons Attribution](https://creativecommons.org/licenses/by/4.0/) License, which permits use, distribution and reproduction in any medium, provided the original work is properly cited.

© 2022 The Authors. *Journal of Applied Polymer Science* published by Wiley Periodicals LLC.

metallic airplane structures, different electrical networks must be developed and implemented in the composite fuselage and other elements of the aircraft, such as the tail cone (electrostatic discharge protection) and wing (electrical conductivity against lightning strikes).<sup>3</sup> CFRP-designed aero-structures need to be multifunctional, with high electrical conductivities comparable to metals and good mechanical performance. Furthermore, the highly conductive fuselage would give ease to the aircraft designer in dealing with challenges like Electromagnetic Interference (EMI), Electromagnetic Shielding (EMS), and Lightning Strike Protection (LSP) on composite fuselage aircraft.

Various techniques have been investigated to increase the through-thickness electrical conductivity of CFRPs. Such techniques include resin modification that involves dispersing conductive materials in a resin matrix, or using a conductive resin,<sup>4-13</sup> modifying carbon fiber surface using grafting, growth, or with chemical treatment,<sup>14-22</sup> or by using interleaves in the composites adding conductive materials between the carbon fiber plies.<sup>23-38</sup> The resin modification method by incorporating conducting nanofillers generally improves the electrical conductivity by order of nine.<sup>39</sup> However, their incorporation causes problems, such as higher resin viscosity, poor fiber wetting, and porosity, leading to poor mechanical properties. The fiber surface modification, which aims to improve interfacial interaction between fiber and the matrix, weakens the fibers, reduces fiber wetting, and decreases stress transfer potential at the fiber-matrix interface.<sup>14</sup>

Interleaving, where a thin interleaving material is inserted between the dry carbon fabric plies or prepreg layers, is a common method for improving the interlaminar fracture toughness and electrical conductivity of CFRPs. Interleaves are also easy to add to the production process. However, the addition of interleaving materials reduces the fiber content and may have a negative impact on the mechanical properties of the laminates.<sup>40</sup>

Vipin Kumar and co-researcher<sup>31</sup> used interleaved multiwall carbon nanotube (MWCNT) buckypaper (BP) to replace resin-rich areas in CFRP laminates. The BP paper interleaved laminates had a through-thickness electrical conductivity of 0.52 S/cm compared to 0.07 S/cm in the control sample. The flexural strength of 1 BP paper interleaved laminate was 581.75 MPa, compared to 584.5 MPa for the control laminate. Flexural strength starts to decline when the number of interleaving BP papers in the laminate increases. The flexural strength of 4 BP paper interleaved laminate was 378.25 MPa. The use of multiwall carbon nanotube (MWCNT) buckypaper (BP) has limited capacity to increase the through-thickness electrical conductivity,

while an increasing number of interleaving BP paper deteriorates the mechanical properties.

Li et al.<sup>41</sup> used polyamide 12 (PA12) films loaded with MWCNT as interleave between carbon fiber prepreg layers to improve the electrical conductivity of CFRP composites. The stacking order of the laminates was  $[0^\circ]_{12}$ , with MWCNT modified PA12 films and unmodified films inserted between each ply. The through-thickness electrical conductivity of control was  $8.6 \times 10^{-5}$  S/cm, and  $1.8 \times 10^{-3}$  S/cm for 10 wt% MWCNTs/PA12 films interleaved samples. The Mode I and Mode II fracture toughness of 10 wt% MWCNT doped film laminates increased by 59.3% and 112.8%, respectively.

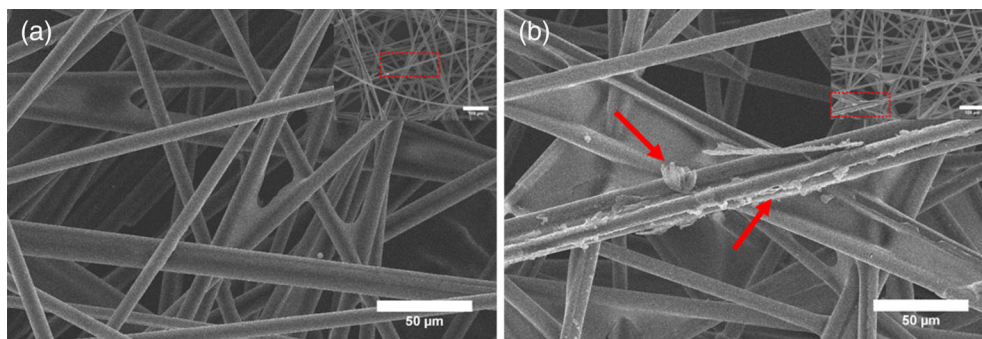
Guo and Yi<sup>42</sup> used AgNW (silver nanowires) coated paper interleaves for improving the electrical conductivity of CFRP composites. The AgNW coated paper interleaved laminates had a through-thickness electrical conductivity of 0.179 S/cm compared to 0.047 S/cm in control samples. Overall the through-thickness electrical conductivity improved, but the Mode I and Mode II interlaminar fracture toughness decreased by 67.3% and 66.9%, respectively. The AgNW coated papers were too densely packed to allow the resin to pass through uniformly, which might have adversely affected the wetting. This indicates that a porous interleave with better resin compatibility could be more useful.

In another work, Guo et al.<sup>43</sup> employed Ag coated interleaves made of nylon and Kevlar veils to increase in-plane and through-thickness electrical conductivity of CFRP composites. The nylon veils were made from long continuous nylon fibers, while the Kevlar veils were made from chopped Kevlar fibers that were randomly placed. The through-thickness electrical conductivity of control was 0.122 S/cm, while for both Ag plated nylon and Kevlar veils, interleaved samples was 3.45 S/cm. The addition of the Ag coated nylon, and Kevlar veil interleaves in the CFRP improved the Mode I (Mode II) fracture toughness by 92% (221%) and by 37% (130%), respectively. The veil interleaves acted as obstacles arresting crack propagation between the plies.

Hu et al.<sup>44</sup> recently used unidirectional carbon fiber and epoxy prepreg along with copper-nickel polyester veils (CNPVs) as functional interlayers. The stacking order of the laminates was  $[+45/0/45/90]_{4s}$ , with CNPVs inserted between each ply. The through-thickness electrical conductivity of the control sample and the CFRP laminate with copper-nickel polyester veils were  $1.5 \times 10^{-3}$  S/cm and 3.25 S/cm, respectively, exhibiting a three order of magnitude improvement. In addition, Mode I and Mode II fracture toughness increased by 59% and 31%, respectively.

Recently Liu et al.<sup>40</sup> reported that a nickel-coated carbon fiber (NiCF) veil improves the electrical conductivity and fracture toughness of carbon fiber/epoxy composites. The unidirectional carbon fiber/epoxy prepregs were

**FIGURE 1** SEM images of (a) CF veil with 14 g/m<sup>2</sup> areal density and 7 μm average fiber diameter and (b) NiCF veil with 20 g/m<sup>2</sup> areal density and 8 μm average fiber diameter [Color figure can be viewed at [wileyonlinelibrary.com](http://wileyonlinelibrary.com)]



used for manufacturing the laminates. A layer of NiCF veil was inserted into mid-plane to fabricate 24 plies unidirectional composite with a layup of  $[0^\circ]_{24}$ . The control sample had  $2.4 \times 10^{-3}$  S/cm through-thickness electrical conductivity, whereas CFRP laminates with NiCF veil of areal densities of 17 g/m<sup>2</sup> and 34 g/m<sup>2</sup> achieved values of  $5.5 \times 10^{-3}$  S/cm and  $7.7 \times 10^{-3}$  S/cm, respectively. Interleaved specimens increased their Mode I and Mode II fracture toughness by 75% and 34%, respectively.

In present article, carbon fiber (CF) and nickel-coated carbon fiber (NiCF) veils were interleaved into CFRP laminates and their effects on through-thickness electrical conductivity, interlaminar shear strength, and flexural strength of the laminates were investigated. A simple hand layup method was used for the fabrication of the laminates. The through-thickness electrical conductivity of the composites specimen was measured using the two-probe method. Mechanical tests including interlaminar shear strength and flexural strength were carried out. The damping properties of the laminates were measured using Dynamic mechanical analysis (DMA). The fracture surfaces were observed using scanning electron microscopy (SEM).

## 2 | MATERIALS AND METHODS

A commercial unidirectional (UD) carbon fiber fabric was used in this study as the dry reinforcement material. The fabric is composed of TENAX J IMS60 E 13 24K fibers in the 0° direction with an areal density of 274 g/m<sup>2</sup> and a glass fiber stitching in 90°. The fabric was supplied by SAERTEX GmbH. The matrix system used in this study was epoxy infusion resin by Easy Composites Ltd., UK, under the brand name of epoxy resin (IN2) (molecular weight = <700 g/mol) mixed with a slow hardener (AT30 slow). Resin to hardener weight ratio of 100:30 was used as recommended by the supplier.

The CF and NiCF veils used in this study are proprietary products of Technical Fiber Products Ltd., UK. The CF veil was made of carbon fiber loosely connected with a cross-linked styrene acrylic binder. The NiCF veil was

made of nickel-coated carbon fiber loosely connected with a cross-linked polyester binder. The SEM images of both the veils are shown in Figure 1. Some nickel particles can be seen (highlighted with red arrows in Figure 1b) adhering to the fiber surface.<sup>40</sup> The random orientation of the veil fibers forms a uniform porous network structure, which aids in resin impregnation. Both the veils were used as received. The areal density, thickness, and average fiber diameter of the CF and NiCF veils are given in Table 1.

### 2.1 | Preparation of composite laminates

To manufacture the unidirectional (UD) laminates, a hand layup process was used with a stack of 5 plies, that is,  $[0]_5$  of carbon fiber fabric, where interleaving veils were placed between each ply. Two laminates were produced for each composition, and a schematic diagram of the laminate fabrication is shown in Figure 2. After the hand layup process, the laminates were consolidated in a press under 1 bar pressure and allowed to cure at ambient temperature for 24 h. The obtained composites were post-cured for 2 h at 40°C and 2 h at 50°C followed by 4 h at 60°C.

### 2.2 | Characterization

The through-thickness electrical conductivity of the composite specimens was measured using the two-probe method.<sup>26</sup> A sample size of 75 × 75 × 1.3 mm was used. The top and bottom surfaces of the laminates were polished to remove the excess epoxy resin and expose the conductive path. A conductive silver epoxy adhesive and hardener (Circuit Works© CW2400) were mixed at a 1:1 ratio and painted onto the plates at nine equally distributed points with 23 AWG copper wire on both sides prior to curing overnight (Figure 3).

A Sciospec ISX-3v2 electrical impedance spectroscopy was used to measure the electrical impedance. One thousand data points were collected for a point electrical resistance in the through-thickness direction.

**TABLE 1** The physical properties, i.e. areal density, dry veil thickness, average fiber diameter, binder type and electrical resistivity of CF and NiCF veils from technical datasheets (Technical Fiber Products Ltd., UK)

Interleaf	Areal density (g/m <sup>2</sup> )	Thickness (μm)	Fiber diameter (μm)	Binder type	Resistivity (Ω/sq.)
Carbon fiber (CF) veil	14	170	7	Cross-linked styrene acrylic	7
Nickel-coated carbon fiber (NiCF) veil	20	180	8	Cross-linked polyester	1.3

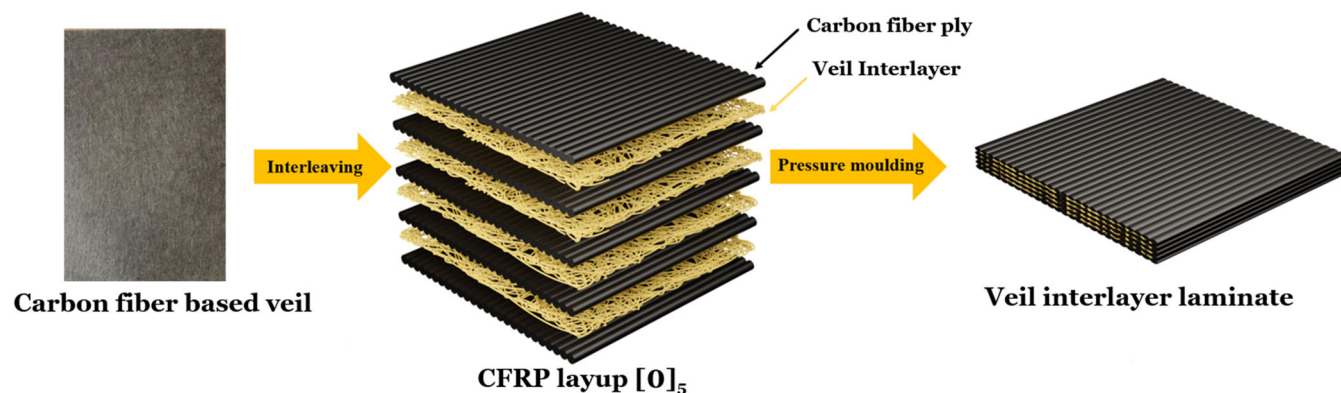


**FIGURE 2** Schematic of overall CF based veil interlayer CFRP laminate preparation [Color figure can be viewed at [wileyonlinelibrary.com](http://wileyonlinelibrary.com)]

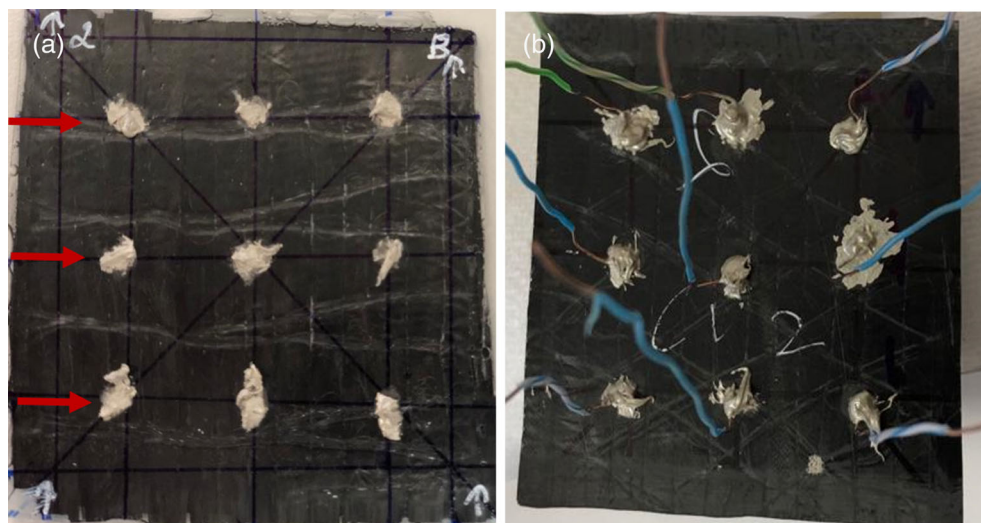


**FIGURE 3** Representative images of the test laminates for through-thickness electrical conductivity measurement (a) conductive silver epoxy applied at nine locations on a laminate, indicated via red arrows and (b) copper wires attached to a laminate [Color figure can be viewed at [wileyonlinelibrary.com](http://wileyonlinelibrary.com)]

The volume conductivity  $\sigma$  was determined by Equation (1)<sup>43,45–48</sup>:

$$\sigma = \frac{1}{\rho} = \frac{L}{RA} \quad (1)$$

where  $\rho$  is the volume resistivity,  $L$  is the thickness of the specimen,  $R$  is the measured electrical resistance of the specimen, and  $A$  is the area of the sample.

Fiber volume fractions (FVF) were determined by the matrix burn-off technique specified in ASTM D3171.

Fiber volume fractions for control, CF veil and NiCF veil-interleaved composites were 59%, 66%, and 63%, respectively.

Interlaminar shear strength was measured by performing short beam shear (SBS) tests. The dimension of the SBS specimens were  $20 \times 10 \times 1.3$  mm, and testing was conducted in accordance with the ISO 14130, where the span to thickness ratio was 15:1. For each laminate, seven samples were tested under a constant displacement rate of 1 mm/min using an Instron 3369 tester.

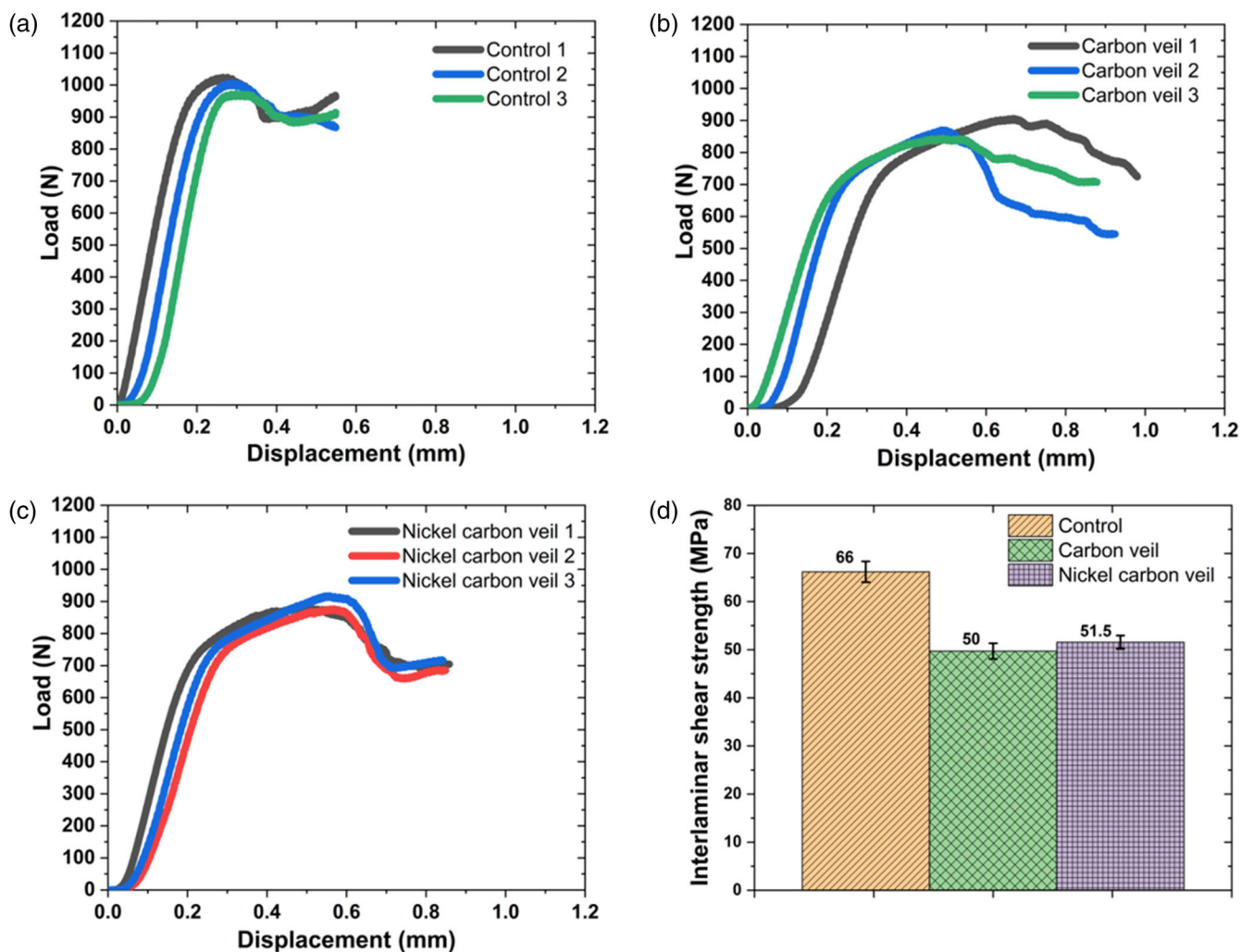


FIGURE 4 Interlaminar shear strength (ILSS) of control and veil-interleaved composites (a–c) load–displacement plots and (d) summary of interlaminar shear strength (ILSS) [Color figure can be viewed at [wileyonlinelibrary.com](http://wileyonlinelibrary.com)]

The flexural properties of specimens were obtained from three-point bend tests, as specified in ISO 14125. For each laminate, five specimens of  $50 \times 15 \times 1.3$  mm were tested. A 5 N pre-load was applied to prevent samples from slipping. Tests were performed using an Instron 3369, with a cross-head displacement of 1 mm/min. Each specimen was loaded until cracks propagated throughout the entire specimen.

Dynamic mechanical analysis (DMA) was performed according to ASTM D4065-12 to investigate the damping properties of the laminates. The test was carried out on samples (dimension:  $35 \times 8 \times 1.3$  mm) using DMA 8000 (Perkin Elmer©) in three-point bending mode, where 20  $\mu$ m displacement amplitudes were applied at 1 Hz. A temperature sweep from 25 to 150°C was used at a heating rate of 5°C/min. Glass transition temperature ( $T_g$ ) and tan delta were determined and plotted using Pyris software to obtain the damping properties of the CFRP.

The fracture surfaces of the CFRP samples from SBS tests were examined by SEM (JSM-IT100, JEOL, Japan) at

an electron excitation voltage of 10 kV. Before the examination, the fracture surfaces were sputter-coated with a thin evaporated layer of gold, until reaching a thickness of approximately 100 Å using an Agar auto sputter coater. The carbon fiber ply and veil interlayer thickness was calculated by taking an average of 50 measurements from different SEM images of SBS samples. The fourier transform infrared spectroscopy (FTIR) ( $4000\text{--}400$   $\text{cm}^{-1}$ ) of the samples was recorded using FTIR spectrometer, Nicolet iS10.

### 3 | RESULTS AND DISCUSSION

#### 3.1 | Interlaminar shear strength and flexural properties

Interlaminar shear strength (ILSS) for the control and veil-interleaved composites samples are plotted in Figure 4. The introduction of the NiCF veils in the interlaminar regions

decreased the shear strength by ca. 22%, from 66 to 51.5 MPa, see Figure 4d. Specimens interleaved with CF veils also exhibited a 24% drop in shear strength compared to the control sample. Pristine CFRP samples exhibited a standard linear trend up to the shear failure, where the ILSS value corresponded to 66 MPa. The interleaved samples showed two distinctive phases. Initially, a stiff response was noted, followed by a second softer behavior, typical to yielding, before failure. It is interesting to note that the interleaved samples experienced a displacement of 0.6 mm until failure, which is about three times greater than the displacement of the control samples. The interlaminar shear strength was lower in the interleaved composites that might be due to weaker interlaminar regions.

The respective stress–strain curves for the flexural tests are shown in Figure 5a–c. The tensile and compressive stresses experienced during flexural testing may cause bending failure, and the effect of shear can be neglected for thin specimens. The flexural stress increased linearly for the control

laminate. These graphs indicate that interleaved veil specimens fail at lower stresses, indicating a sudden loss of load carrying capacity. Flexural testing revealed that the veil samples have lower flexural strength than the control specimens by 20% for the CF veil and 23% for the NiCF veil, as shown in Figure 5d. Interleaving causes a reduction in flexural performance of CFRP, since the embedded veil has a lower stiffness and strength. The flexural strength of both veil-interleaved laminates is almost equal. Yuan and Bard<sup>49,50</sup> also reported that the interlayer had a negative impact on the flexural strength of the laminates regardless of the interlayer fiber type, diameter, or length.

### 3.2 | Dynamic mechanical properties

The dynamic mechanical properties of the interleaved laminates were evaluated in three-point bend mode. The  $\tan\delta$  (damping parameter) results are shown in Figure 6

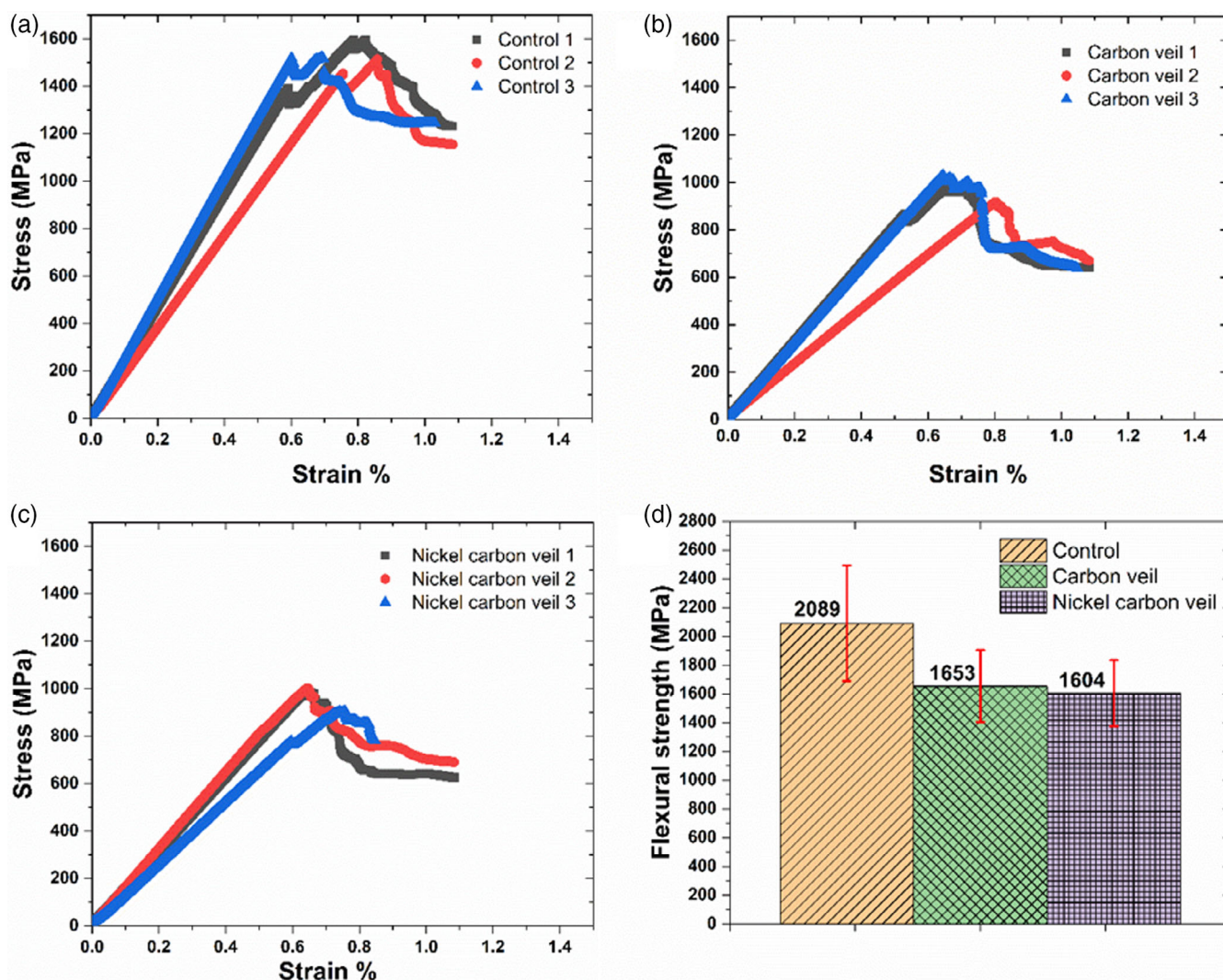
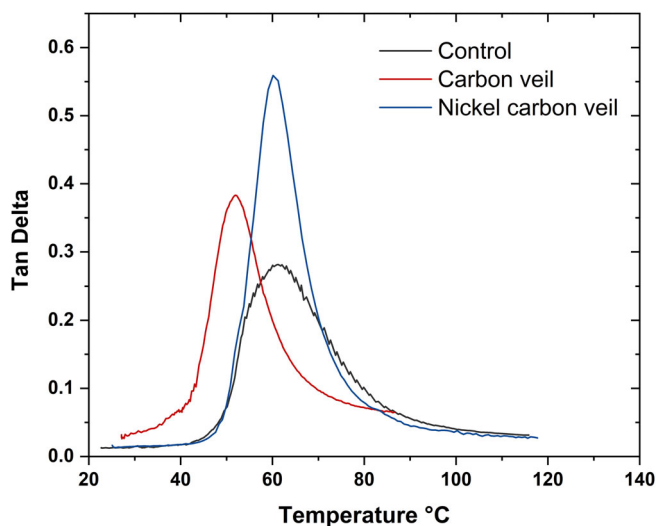


FIGURE 5 Flexural properties of control and veil-interleaved composites (a–c) flexural stress–strain plots and (d) summary of flexural strength [Color figure can be viewed at [wileyonlinelibrary.com](http://wileyonlinelibrary.com)]



**FIGURE 6** Tan $\delta$  of control and veil-interleaved composite samples in temperature sweep [Color figure can be viewed at [wileyonlinelibrary.com](http://wileyonlinelibrary.com)]

as a function of temperature. The tan $\delta$  is the ratio of the viscous response to the elastic response of the material. The tan $\delta$  peak height, breadth, and glass transition temperature of the interleaved laminates were compared with the control laminate in Figure 6. The highest tan $\delta$  peak was observed in NiCF veil-interleaved CFRP samples, followed by CF veil-interleaved and control samples. Tan $\delta$  refers to the internal energy dissipation within the material. The tan $\delta$  height for interleaved samples was higher compared to the control CFRP but with narrower peaks, indicating that the CFRP had a stronger fiber-matrix interface. The presence of binders and Ni coating on the CF veils might have an adverse effect on the bonding of epoxy resin with the veils. This resulted in higher chain mobility leading to higher energy dissipation, as seen with higher tan $\delta$  peak heights.

### 3.3 | Fourier transform infrared spectroscopy

FTIR spectra of control, CF veil and NiCF veil-interleaved composites are shown in Figure 7. The binder present on the CF veil is cross-linked styrene-acrylic resin. In the CF veil-interleaved composite, the peak at 1727  $\text{cm}^{-1}$  might be attributed to the C=O stretching of the ester side group of the acrylic component in the binder.<sup>51</sup> But the binder is hydrophobic in nature and is not likely to have any interaction with the hydrophilic epoxy resin. On the other hand, NiCF veil has a cross-linked polyester resin as the binder. The ester linkages present in the backbone of the polyester resin might have

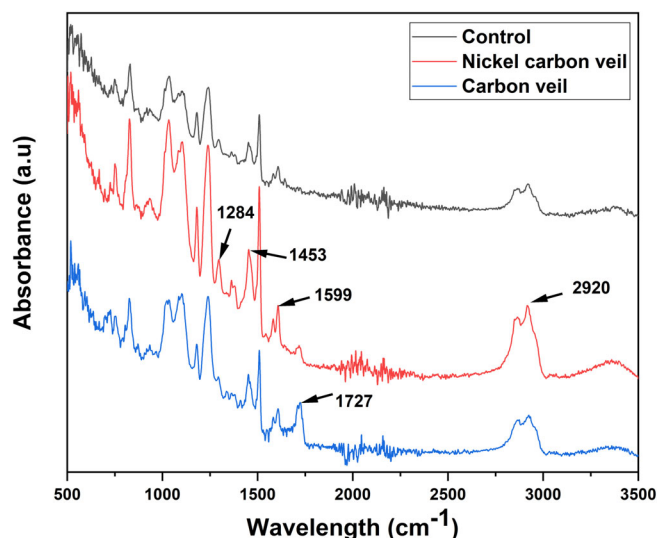


**FIGURE 7** FTIR spectra of control and veil-interleaved composites [Color figure can be viewed at [wileyonlinelibrary.com](http://wileyonlinelibrary.com)]

an H-bonding interaction with the OH groups of the epoxy resin. The OH stretching vibrations of the cured epoxy resins are observed in the range of 3200–3500  $\text{cm}^{-1}$  in all the samples. The prominent peak observed at 2920  $\text{cm}^{-1}$  in the NiCF veil-interleaved composite might be attributed to the stretching vibration of C—H bond in aromatic hydrocarbons in the cross-linked polyester binder. The ring skeleton vibration absorption peak at 1599  $\text{cm}^{-1}$  represents the stretching vibration of the C=C bond in the benzene ring, consistent with the characteristic peak of polyester resin reported in the literature.<sup>52,53</sup> The band at 1284  $\text{cm}^{-1}$  in the spectrum of polyester is caused by the twisting and vibration of the CH<sub>2</sub> groups.<sup>54</sup> The presence of binders are therefore evident in the FTIR analysis. But binders are generally present in very small amounts on the veils (Figure 1) and in this study, they are not chemically compatible with the epoxy resin. Hence, they are not likely to play any role in changing the interaction between the veil and the matrix resin. This is supported by the fact that the ILSS values observed were very similar in both the interleaved composites and the ILSS values were lower than the control laminate.

### 3.4 | SEM analysis

The SEM images of the interleaved laminates show that the veil interlayers are almost parallel to the carbon fiber plies and create a periodically laminated structure (see orange dashed lines in Figure 8). The carbon fiber plies and veil interlayers are well compacted, albeit some voids and imperfections can be seen, specifically within the veil



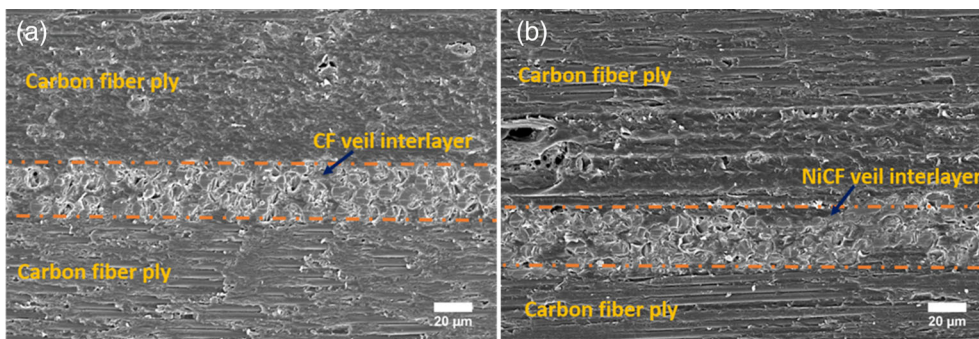


**FIGURE 8** Representative SEM images of as prepared veil-interleaved composites in a longitudinal direction (a) CF veil and carbon fiber ply in CF veil-interleaved composites and (b) NiCF veil and carbon fiber ply in NiCF veil-interleaved composites (note that images are captured from the  $x$ - $y$  plane and the position of the veils is given by the orange dashed lines) [Color figure can be viewed at [wileyonlinelibrary.com](http://wileyonlinelibrary.com)]

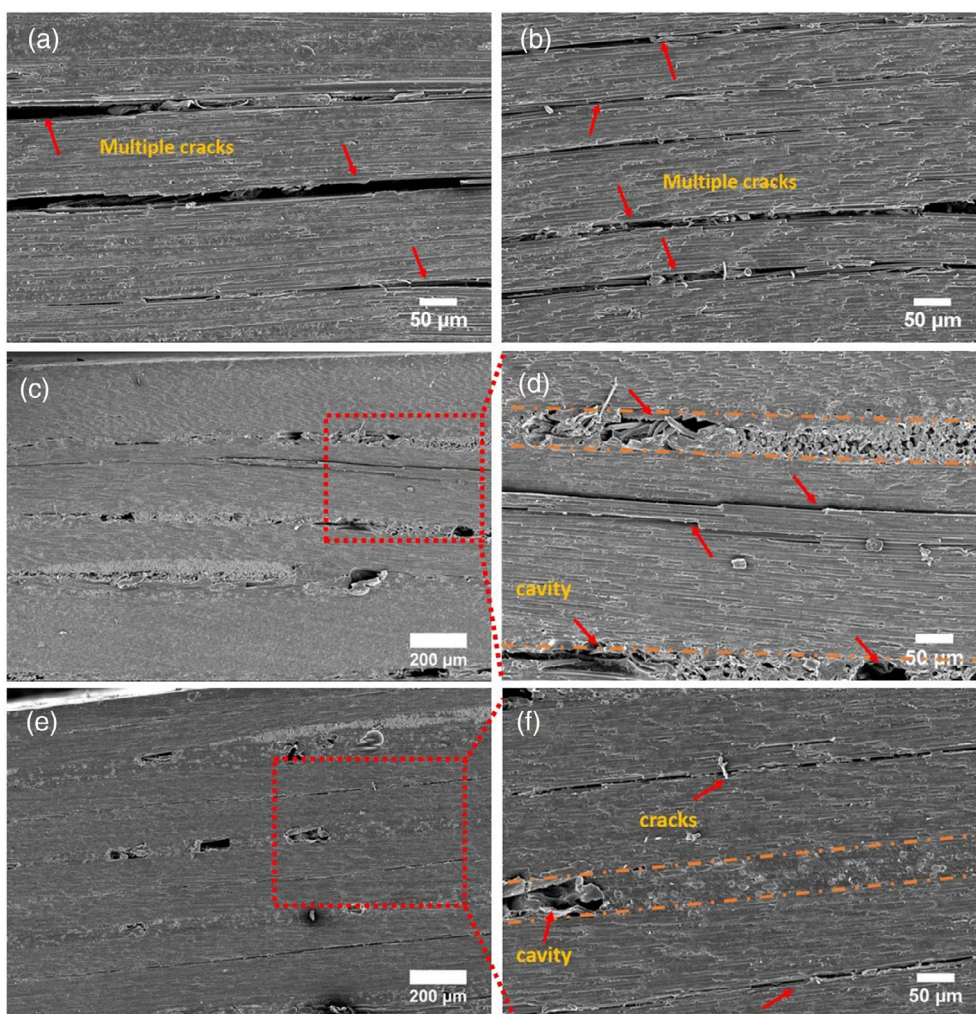


**FIGURE 9** Representative SEM images of ILSS tested samples in a longitudinal direction (a, b) control (c, d) CF veil-interleaved composites, and (e, f) NiCF veil-interleaved composites (note that images are captured from the  $x$ - $y$  plane, and the position of the veils is given by the orange dashed lines) [Color figure can be viewed at [wileyonlinelibrary.com](http://wileyonlinelibrary.com)]

interlayer regions. The veil to fabric thickness ratios remained the same throughout the composite thickness. The average thickness of the carbon fiber ply in CF veil-interleaved laminate is around ca.  $235 \pm 37 \mu\text{m}$ , and the CF veil interlayer thickness is ca.  $50 \pm 4 \mu\text{m}$ . In the NiCF veil-interleaved laminate, the average thickness of carbon

fiber ply is ca.  $226 \pm 24 \mu\text{m}$ , and the NiCF veil interlayer is ca.  $56 \pm 4.6 \mu\text{m}$ .

The failed ILSS specimens were examined under SEM to determine their failure behavior. The fracture surfaces of a pristine CFRP exhibited brittle behavior, as shown in Figure 9a, b. Multiple shear fractures can be seen after

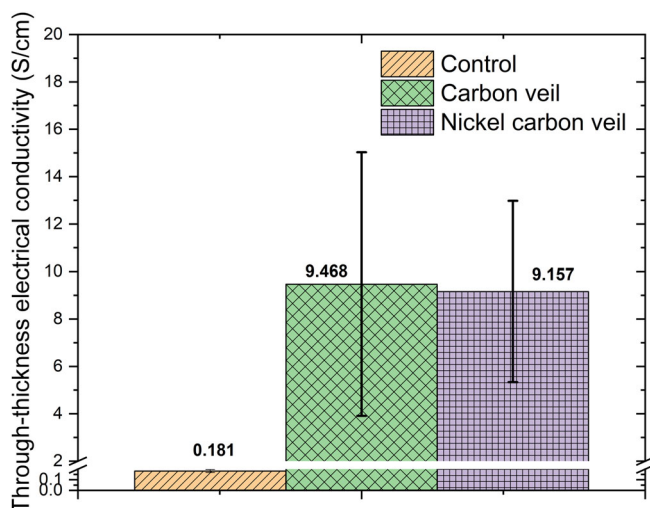


**FIGURE 10** Through-thickness electrical conductivity of control, CF and NiCF veil-interleaved CFRP composites. Veil interlayer laminates have a ca. 51 fold increase in electrical conductivity compared to the control specimen [Color figure can be viewed at [wileyonlinelibrary.com](http://wileyonlinelibrary.com)]

the ILSS test. The fracture surfaces of the veil-interleaved CFRPs in Figure 9c–f show a noticeable difference as compared to the control laminate. The number and extension of cracks in the interleaved laminates are diminished. This might be due to the fact that the veil fibers take part in energy absorption in the interlayer region. The cracks in the matrix of the veil-interleaved laminates are shown by the red arrows. Some voids and cavities can be seen in the veil-interleaved regions (Figure 9d and f). These might be caused due to random orientation of the veil fibers, which forms a porous network. As the areal density increases, the probability of weak points through the veil also increases and presumably stress transfer efficiency also decreases because of added weak interlayer with lower stiffness, which is likely responsible for the reduction in mechanical properties.<sup>44,50,55</sup>

### 3.5 | Through-thickness electrical conductivity

The through-thickness electrical conductivity of the CF/epoxy laminates interleaved with CF veil or NiCF veils were measured and compared to the control CFRP as reference. The average through-thickness electrical conductivity of the interleaved laminates was ca. 51 times higher, from 0.181 S/cm for the control CFRP sample to 9.46 S/cm for the CF veil-interleaved laminates see Figure 10. The conductivity of the NiCF veil-interleaved composite, on the other hand, was found to be

9.16 S/cm. This substantial increase in through-thickness electrical conductivity was attributed to the presence of the conductive veil interlayers

The spacing between the particles is crucial for electron transport for heterogeneous materials. With the inclusion of the conductive veils, the electron's ability to jump throughout the entire sample from one interlayer to the next was considerably boosted by following the least resistance path. The sudden rise in electrical conductivity due to incorporation of conductive veils in the interlayer regions indicates that the percolation threshold has been reached. Because of the porous nature of veil, the conductive paths replace the conventional resin-rich regions in the interlaminar area and break the insulating barriers in through-thickness directions.<sup>44,50,55</sup>

According to Brown et al.,<sup>46</sup> a highly conductive interlayers would improve overall conductivity. However, the bulk conductivity of carbon fibers, the composite's volume fraction, and the structural characteristics of conductive interleaves (thickness and areal density) also play an essential role. The matrix interpenetration into the interleaves is important for electrical conductivity and mechanical properties. The NiCF veil has a higher areal density than the CF veil (see Table 1). Therefore, resin-rich zones might exist above and below a denser interleave that does not create an inter-penetrative network with the insulating resin. As a result, when compared to CF veil-interleaved composite, the laminate interleaved with NiCF veil has a slightly reduced through-thickness electrical conductivity. Another reason for this behavior is because the average thickness of the NiCF veil interlayer is marginally higher (ca. 6  $\mu\text{m}$ ) compared to the CF veil interlayer that might have influenced the continuous electrical pathway.

## 4 | CONCLUSION

CFRP composites were produced with interleaved CF or NiCF veils. A hand layup technique was used for the fabrication of the composites. The interleaved conductive veils incorporated in the resin-rich interlaminar regions between the carbon fiber plies improved the through-thickness electrical conductivity of the laminates. The through-thickness electrical conductivities of CF and NiCF interleaved composites increased from 0.181 (control) to 9.46 and 9.16 S/cm, respectively. The interlaminar shear strength was reduced by ca. 22%–24% compared to that of the control specimen. The control sample underwent extensive shear failures at multiple locations, but the interleaved composites did not follow this pattern. Although electrical conductivities were enhanced, the incorporation of veils might have induced some

weakness in the interlaminar regions, leading to a drop in the mechanical properties. This drop can be minimized with a suitable reactive binder on the veils and by keeping the veil areal weight as low as possible. The results show that the CF or NiCF veil based CFRPs composites can provide a cost-effective and efficient way to meet the structural and functional integration requirements of the aerospace industry for electrical properties, presenting a wide range of potential applications in the field of lightning protection, EMI shielding, and structural health monitoring.

## AUTHOR CONTRIBUTIONS

**Muhammad Waqas:** Conceptualization (lead); data curation (lead); formal analysis (lead); investigation (lead); methodology (lead); validation (lead); writing – original draft (lead); writing – review and editing (lead). **Colin Robert:** Formal analysis (supporting); writing – review and editing (supporting). **Urwah Arif:** Resources (supporting); writing – review and editing (supporting). **Norbert Radacsi:** Investigation (supporting); writing – review and editing (supporting). **Dipa Ray:** Supervision (supporting) concept of using conducting veils, writing – review and editing (supporting). **Vasileios Koutsos:** Supervision (lead); writing – review and editing (lead).

## ACKNOWLEDGMENTS

The first author would like to thank Higher Education Commission (HEC), Pakistan, for their financial support. We would like to acknowledge Technical Fiber Products Ltd., UK for providing the veil samples. The authors also like to thank Mr. Edward Monteith and Miss Katalin Kis for their support. For the purpose of open access, the author has applied a Creative Commons Attribution (CC BY) license to any Author Accepted Manuscript version arising from this submission.


## DATA AVAILABILITY STATEMENT

The data that support the findings of this study are available in the supplementary material of this article.

## ORCID

Muhammad Waqas  <https://orcid.org/0000-0002-1251-0492>

Dipa Ray  <https://orcid.org/0000-0002-2353-9581>

Vasileios Koutsos  <https://orcid.org/0000-0002-2203-8179>

## REFERENCES

- [1] S. Wang, Z. Mei, D. D. L. Chung, *Int. J. Adhes. Adhes.* **2001**, *21*, 465.
- [2] O. G. Kravchenko, D. Pedrazzoli, V. S. Bonab, I. Manas-Zloczower, *Mater. Des.* **2018**, *160*, 1217.
- [3] L. Ye, *Natl. Sci. Rev.* **2014**, *1*, 7.
- [4] Z. Fan, M. H. Santare, S. G. Advani, *Compos. Part A: Appl. Sci. Manufact.* **2008**, *39*, 540.
- [5] G. W. Beckermann, *Reinforced Plastics* **2017**, *61*, 289.
- [6] Y. Wang, S. K. R. Pillai, J. Che, M. B. Chan-Park, *ACS Appl. Mater. Interfaces* **2017**, *9*, 8960.
- [7] X. Han, Y. Zhao, J.-m. Sun, Y. Li, J.-d. Zhang, Y. Hao, *New Carbon Mater.* **2017**, *32*, 48.
- [8] X. Cheng, T. Yokozeki, L. Wu, H. Wang, J. M. Zhang, J. Koyanagi, Z. Weng, Q. Sun, *Compos. Part A: Appl. Sci. Manufact.* **2016**, *90*, 243.
- [9] M. Tehrani, M. Safdari, A. Y. Boroujeni, Z. Razavi, S. W. Case, K. Dahmen, H. Garmestani, M. S. Al-Haik, *Nanotechnology* **2013**, *24*, 155704.
- [10] M. Tehrani, A. Y. Boroujeni, T. B. Hartman, T. P. Haugh, S. W. Case, M. S. Al-Haik, *Compos. Sci. Technol.* **2013**, *75*, 42.
- [11] F. H. Gojny, M. H. G. Wichmann, B. Fiedler, W. Bauhofer, K. Schulte, *Compos. Part A: Appl. Sci. Manufact.* **2005**, *36*, 1525.
- [12] Li. Danning, J. Barrington, S. James, D. Ayre, M. Słoma, M.-F. Lin, H. Y. Nezhad, *Sci. Rep.* **2022**, *12*, 7504.
- [13] K. R. Reddy, B. Hemavathi, G. R. Balakrishna, A. V. Raghu, S. Naveen, M. V. Shankar, in *Polymer Composites with Functionalized Nanoparticles* (Eds: K. Pielichowski, T. M. Majka), Elsevier, Oxford, UK **2019**, p. 357.
- [14] H. S. Bedi, S. S. Padhee, P. K. Agnihotri, *Polym. Compos.* **2018**, *39*, E1184.
- [15] M. Delamar, G. Desarmot, O. Fagebaume, R. Hitmi, J. Pinsonc, J.-M. Savéant, *Carbon* **1997**, *35*, 801.
- [16] T. R. Pozegic, I. Hamerton, J. V. Anguita, W. Tang, P. Ballocci, P. Jenkins, S. R. P. Silva, *Carbon* **2014**, *74*, 319.
- [17] C. Robert, W. B. Thitasiri, D. Mamalis, Z. E. Hussein, M. Waqas, D. Ray, N. Radacsi, V. Koutsos, *J. Appl. Polym. Sci.* **2020**, *138*, 49749.
- [18] F. Yan, L. Liu, M. Li, M. Zhang, L. Shang, L. Xiao, Y. Ao, *Compos. Part A: Appl. Sci. Manufact.* **2019**, *125*, 105530.
- [19] P. K. Gangineni, S. Yandrapu, S. K. Ghosh, A. Anand, R. K. Prusty, B. C. Ray, *Compos. Part A: Appl. Sci. Manufact.* **2019**, *122*, 36.
- [20] H. Yao, G. Zhou, W. Wang, M. Peng, *Compos. Struct.* **2018**, *195*, 288.
- [21] J. K. Park, J. Y. Lee, L. T. Drzal, D. Cho, *Carbon Lett.* **2016**, *17*, 33.
- [22] W. Qin, F. Vautard, L. T. Drzal, Y. Junrong, *Composites, Part B* **2015**, *69*, 335.
- [23] M. S. Sohn, X. Z. Hu, J. K. Kim, L. Walker, *Composites, Part B* **2000**, *31*, 681.
- [24] B. Beylergil, M. Tanoğlu, E. Aktaş, *J. Appl. Polym. Sci.* **2017**, *134*, 45244.
- [25] S. Van der Heijden, L. Daelemans, B. De Schoenmaker, I. De Baere, H. Rahier, W. Van Paeppegem, K. De Clerck, *Compos. Sci. Technol.* **2014**, *104*, 66.
- [26] P. Koirala, N. van de Werken, L. Hongbing, R. H. Baughman, R. Ovalle-Robles, M. Tehrani, *Composites, Part B* **2021**, *216*, 108842.
- [27] K. Aruchamy, A. Mahto, S. K. Nataraj, *Nano-Struct. Nano-Objects* **2018**, *16*, 45.
- [28] G. Wang, Y. Demei, A. D. Kelkar, L. Zhang, *Prog. Polym. Sci.* **2017**, *75*, 73.
- [29] M. Guo, X. Yi, *Carbon* **2013**, *58*, 241.

- [30] S. M. García-Rodríguez, J. Costa, K. E. Rankin, R. P. Boardman, V. Singery, J. A. Mayugo, *Compos. Part A: Appl. Sci. Manufact.* **2020**, *128*, 105659.
- [31] V. Kumar, S. Sharma, A. Pathak, B. P. Singh, S. R. Dhakate, T. Yokozeki, T. Okada, T. Ogasawara, *Compos. Struct.* **2019**, *210*, 581.
- [32] G. W. Beckermann, K. L. Pickering, *Compos. Part A: Appl. Sci. Manufact.* **2015**, *72*, 11.
- [33] M. Guo, X. Yi, G. Liu, L. Liu, *Compos. Sci. Technol.* **2014**, *97*, 27.
- [34] Y. Wu, X. Cheng, S. Chen, Q. Bo, R. Wang, D. Zhuo, L. Wu, *Mater. Des.* **2021**, *202*, 109535.
- [35] K. Dydek, A. Boczkowska, P. Latko-Durałek, M. Wilk, K. Padykuła, R. Kozera, *J. Compos. Mater.* **2020**, *54*, 2677.
- [36] D. Quan, C. Mischo, X. Li, G. Scarselli, A. Ivanković, N. Murphy, *Compos. Sci. Technol.* **2019**, *182*, 107775.
- [37] G. Ognibene, A. Latteri, S. Mannino, L. Saitta, G. Recca, F. Scarpa, G. Cicala, *Polymers (Basel)* **2019**, *11*, 1029.
- [38] L. Q. Cortes, S. Racagel, A. Lonjon, E. Dantras, C. Lacabanne, *Compos. Sci. Technol.* **2016**, *137*, 159.
- [39] W. Bauhofer, J. Z. Kovacs, *Compos. Sci. Technol.* **2009**, *69*, 1486.
- [40] H. Liu, Y. Guo, Y. Zhou, G. Wan, Z. Chen, Y. Jia, *Polym. Compos.* **2021**, *42*, 5335.
- [41] W. Li, D. Xiang, L. Wang, E. Harkin-Jones, C. Zhao, B. Wang, Y. Li, *RSC Adv.* **2018**, *8*, 26910.
- [42] M. Guo, X. Yi, *Aerospace* **2018**, *5*, 77.
- [43] M. Guo, X. Yi, C. Rudd, X. Liu, *Compos. Sci. Technol.* **2019**, *176*, 29.
- [44] D. Hu, X. Yi, M. Jiang, G. Li, X. Cong, X. Liu, C. Rudd, *Aerospace Sci. Technol.* **2020**, *98*, 105669.
- [45] R. Prabhu, T. Jeevananda, K. R. Reddy, A. V. Raghu, *Mater. Sci. Energy Technol.* **2021**, *4*, 1076.
- [46] S. C. Brown, C. Robert, V. Koutsos, D. Ray, *Compos. Part A: Appl. Sci. Manufact.* **2020**, *133*, 105885.
- [47] D. D. L. Chung, in *Carbon Composites*, Elsevier Inc, Oxford, UK **2017**, p. 161.
- [48] D. A. Nguyen, A. V. Raghu, J. T. Choi, H. M. Jeong, *Polym. Polym. Compos.* **2010**, *18*, 351.
- [49] B. Yuan, M. Ye, H. Yunsen, F. Cheng, X. Hu, *Compos. Part A: Appl. Sci. Manufact.* **2020**, *131*, 105813.
- [50] S. Bard, F. Schön, M. Demleitner, V. Altstädt, *Polymers* **2019**, *11*, 823.
- [51] F. Jia, E. O. Fagbohun, Q. Wang, D. Zhu, J. Zhang, B. Gong, Y. Cui, *Carbon Resour. Convers.* **2021**, *4*, 190.
- [52] V. Cecen, Y. Seki, M. Sarikanat, I. H. Tavman, *J. Appl. Polym. Sci.* **2008**, *108*, 2163.
- [53] M. G. González, J. C. Cabanelas, J. Baselga, *Infrared Spectrosc. Mater. Sci. Eng. Technol.* **2012**, *2*, 261.
- [54] M. Chukwu, C. Madueke, L. Ekebafé, *Niger. Res. J. Chem. Sci.* **2019**, *6*, 21.
- [55] V. A. R. Elias, in *School of Materials*, University of Manchester, UK, **2015**, 287.

## SUPPORTING INFORMATION

Additional supporting information can be found online in the Supporting Information section at the end of this article.

**How to cite this article:** M. Waqas, C. Robert, U. Arif, N. Radacsi, D. Ray, V. Koutsos, *J. Appl. Polym. Sci.* **2022**, e53060. <https://doi.org/10.1002/app.53060>